Materials Science in Semiconductor Processing 169 (2024) 107870

Contents lists available at ScienceDirect

Materials Science in Semiconductor Processing

journal homepage: www.elsevier.com/locate/mssp

Full length article

TCAD modelling of a-Si:H devices for particle detection applications

Daniele Passeri [a,b,*], Arianna Morozzi [b], Michele Fabi [e,d], Catia Grimani [e,d], Stefania Pallotta [c,d], Federico Sabbatini [e,d], Cinzia Talamonti [c,d], Mattia Villani [e,d], Lucio Calcagnile [f,g], Anna Paola Caricato [f,g], Maurizio Martino [f,g], Giuseppe Maruccio [f,g], Anna Grazia Monteduro [f,g], Gianluca Quarta [f,g], Silvia Rizzato [f,g], Roberto Catalano [h], Giuseppe Antonio Pablo Cirrone [h], Giacomo Cuttone [h], Giada Petringa [h], Luca Frontini [i], Valentino Liberali [i], Alberto Stabile [i], Tommaso Croci [b], Maria Ionica [b], Keida Kanxheri [b,j], Mauro Menichelli [b], Francesco Moscatelli [b,k], Maddalena Pedio [b,k], Francesca Peverini [b,j], Pisana Placidi [a,b], Luca Tosti [b], Giulia Rossi [b], Leonello Servoli [b], Nicola Zema [b,l], Giovanni Mazza [m], Lorenzo Piccolo [m], Richard Wheadon [m], Luca Antognini [n], Sylvain Dunand [n], Nicolas Wyrsch [n], Aishah Bashiri [o], Matthew Large [o], Marco Petasecca [o]

[a] University of Perugia, Department of Engineering, Via G. Duranti 93, 06125, Perugia, Italy
[b] INFN Sezione di Perugia, Via Pascoli, 06123 Perugia, Italy
[c] Università degli Studi di Firenze, Dip. di Fisica Scienze Biomediche Sperimentali e Cliniche, Viale Morgagni 50, 50135 Firenze (FI), Italy
[d] INFN Sezione di Firenze, Via Bruno Rossi, 1, 50019 Sesto Fiorentino FI Firenze (FI), Italy
[e] DiSPeA, Università di Urbino Carlo Bo, 61029 Urbino (PU), Italy
[f] Department of Mathematics and Physics "Ennio de Giorgi" University of Salento, Via per Arnesano, 73100 Lecce, Italy
[g] INFN Sezione di Lecce, Via Provinciale per Arnesano, 73100 Lecce, Italy
[h] INFN Laboratori Nazionali del Sud, Via S.Sofia 62, 95123 Catania, Italy
[i] INFN Sezione di Milano, Via Celoria 16, 20133 Milano, Italy
[j] Dip. di Fisica e Geologia dell'Università degli Studi di Perugia, via Pascoli s.n.c. 06123 Perugia, Italy
[k] CNR-IOM, via Pascoli s.n.c. 06123 Perugia, Italy
[l] CNR Istituto struttura della Materia, Via Fosso del Cavaliere 100, Roma, Italy
[m] INFN Sezione di Torino Via Pietro Giuria, 1, 10125 Torino, Italy
[n] Ecole Polytechnique Fédérale de Lausanne (EPFL), Photovoltaic and Thin-Film Electronics Laboratory (PV-Lab), Rue de la Maladière 71b, 2000 Neuchâtel, Switzerland
[o] Centre for Medical Radiation Physics, University of Wollongong, Northfields Ave Wollongong NSW 2522, Australia

ARTICLE INFO

Keywords:
TCAD
Amorphous silicon
Particle detectors
Device simulation

ABSTRACT

Hydrogenated amorphous silicon (a-Si:H) has been proposed as a suitable material for particle detection applications thanks to its property to be deposited over a large area and above a variety of different substrates, including flexible materials. Moreover, the low cost and intrinsic radiation tolerance made this material appealing in applications where high fluences are expected, e.g. in high energy physics experiments. In order to optimize the device geometry and to evaluate its electrical behaviour in different operating conditions, a suitable Technology CAD (TCAD) design methodology can be applied. In this work, carried out in the framework of the HASPIDE INFN project, we propose an innovative approach to the study of charge transport within the material, using the state-of-the-art Synopsys Advanced TCAD Suite. Different custom mobility models have been devised and implemented within the code as external PMI (Physical Model Interfaces), starting from the Poole–Frenkel model and accounting for different dependencies on temperature and internal potential distribution, thus resulting in a new mobility model embedded within the code. Simple test structures, featuring p-i-n diodes have been simulated and compared to experimental data as a benchmark. The overall aim was to account for the effect of different biasing conditions (namely, different electrical potential and electric field distribution within the device) and operating conditions (e.g. temperature). This work fosters the use of commercially available TCAD suite such as Synopsys Sentaurus, largely diffused in the radiation detection scientific community, for the design and optimization of innovative a-Si:H devices for particle detection applications.

* Corresponding author at: University of Perugia, Department of Engineering, Via G. Duranti 93, 06125, Perugia, Italy.
E-mail address: daniele.passeri@unipg.it (D. Passeri).
URL: https://www.unipg.it/personale/daniele.passeri/en/ (D. Passeri).

https://doi.org/10.1016/j.mssp.2023.107870
Received 3 August 2023; Received in revised form 20 September 2023; Accepted 26 September 2023
Available online 7 October 2023

1. Introduction

Hydrogenated amorphous silicon (a-Si:H) has been proposed as a suitable material for particle detection applications thanks to its property to be deposited over a large area and above a variety of different substrates, including flexible materials. Moreover, the low cost and intrinsic radiation tolerance made this material appealing in applications where high fluences are expected, e.g. in high energy physics experiments. In order to optimize the device geometry and to evaluate its electrical behaviour in different operating conditions, a suitable Technology CAD (TCAD) design methodology can be applied. In this work, carried out in the framework of the HASPIDE INFN project [1], we propose an innovative approach to the study of charge transport within the material, using the state-of-the-art Synopsys Advanced TCAD Suite. To this purpose, a dedicated, new material parametrization to model the behaviour of a-Si:H within the Sentaurus TCAD material library has been included [2,3]. An extensive selection of acceptor and donor defects (acting as traps and/or recombination centres) within the band-gap has been considered, along with different options of energy distributions. The main parameters taken into account are defects energy level, capture cross-sections, and traps density and occupancy. The defects' impact on the device's electrical behaviour has been simulated, e.g. by changing the type and concentration of defects and by varying the material Fermi's level position. Different charge transport models have been compared, from the classic drift-diffusion to the thermodynamic and hydrodynamic approximations.

In particular, different custom mobility models have been devised and implemented within the code as external PMI (Physical Model Interfaces), starting from the Poole–Frenkel model and accounting for different dependencies on carrier concentrations, temperature and internal potential distribution.

Test structures, featuring p-i-n diodes have been simulated and the results compared to experimental data as a benchmark. The overall aim was to devise a device-level modelling approach to be exploited in particle detector design, accounting for the effect of different biasing conditions (namely, different electrical potential and electric field distribution within the device) and operating conditions (e.g. temperature). Capacitance vs. voltage small-signal simulations and measurements analyses have been carried out to validate the model parametrization, while current vs. voltage simulations and measurements comparison has been used to check the suitability of the proposed charge transport and mobility models.

2. TCAD modelling of a-Si:H

Technological Computer Aided Design (TCAD) tools are routinely adopted within the design flow of conventional solid-state devices, given the availability of material properties description (in particular for mono-crystalline Silicon) and extensive sets of models for device physics and effects in semiconductor devices (e.g. drift-diffusion, thermodynamic, and hydrodynamic models). Even non conventional devices and their applications can be considered, e.g. silicon detectors for particle tracking, where operating conditions such as extremely high biasing and high electric field regions, as well as radiation damage effects, have to be accounted for.

However, given the large variance in reported properties for a-Si:H, there is at present no established commercial model and methodologies of this material available to truly mimic the electrical and charge collection behaviour of hydrogenated amorphous silicon within the context of ionizing radiation detection applications. Actually, the vast majority of device-level simulation based studies dealing with a-Si:H are primarily concerned with thin film devices (i.e., nm thickness range) for photovoltaic applications [4–7].

In this work, we rely on the state-of-the-art SYNOPSYS© Sentaurus TCAD simulation tool which was developed primarily for design and fabrication optimization of semiconductor electronic devices [8]. Given

```
...
# Tail for Donor
(Donor Level EnergyMid=0.00 fromValBand
     Conc = @<8.77e20*DonIntroFac>@ eXsection=1e-14 hXsection=1e-16 Add2TotalDoping)
(Donor Level EnergyMid=0.15 fromValBand
     Conc = @<4.09e19*DonIntroFac>@ eXsection=1e-14 hXsection=1e-16 Add2TotalDoping)
(Donor Level EnergyMid=0.30 fromValBand
     Conc = @<1.67e18*DonIntroFac>@ eXsection=1e-14 hXsection=1e-16 Add2TotalDoping)
...
```

Fig. 1. Trap specification within the Physics section of the command file - Sentaurus sdevice tool.

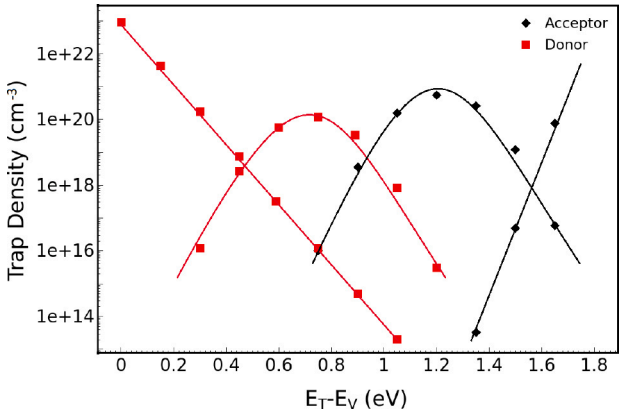

Fig. 2. Overall defects concentration of conduction and valence band tail states (straight lines) and deep-level Gaussian states within the a-Si:H material.

that a-Si:H is not available within the standard material libraries, users interested in simulating a-Si:H based devices are forced to develop their own material models to reproduce the material behaviour in the operating conditions of interest (e.g. biasing and temperature). Despite the significant differences within the structure of c- Si and a-Si:H, only a few major parameters within the new material parameter file were required to be modified, such as the low field electron and hole mobilities and the adjustment of the band-gap [3].

A key point in this study is appropriately modelling various deep-level defects within the a-Si:H band-gap that can act as recombination centres and/or trap states. Defect density or concentration of conduction and valence band tail states and deep-level Gaussian states within the a-Si:H material can be specified, following multiple, trap states introductions. This approach has been well assessed for modelling the effects of radiation damage (e.g., displacement and ionizing effects) in silicon substrates and silicon interfaces [9–11].

Traps can be categorized in acceptor-type (uncharged when unoccupied, negatively charged when occupied) and donor-type (uncharged when unoccupied, positively charged when occupied) depending on their behaviour when the charge is present, but it is possible to define multiple energetic distribution methods to define their spatial positioning. Within Sentaurus sdevice it is possible to implement the Single Level, Uniform, Exponential, Gaussian (and even a random distribution in the trap specification) as traps' energetic and spatial distributions. In this work, we refer to multiple, single-levels energy distribution. Besides the energy level, each trap can be specified in terms of type (acceptor or donor), capture cross-sections and concentration within the material. A typical trap description of a single-acceptor level within the code is reported in Fig. 1, while the overall defects concentration of conduction and valence band tail states (straight lines) and deep-level Gaussian states is reported in Fig. 2. Proper introduction rates (*IntroFac*) can be also specified for classes of trap type (e.g. tails or Gaussian), thus controlling the effectiveness of the traps themselves.

The resulting carrier concentrations, e.g. the effective charge concentration depending on the occupation probabilities of the defect level is determined by the Fermi-Dirac statistics, e.g. by the Fermi's

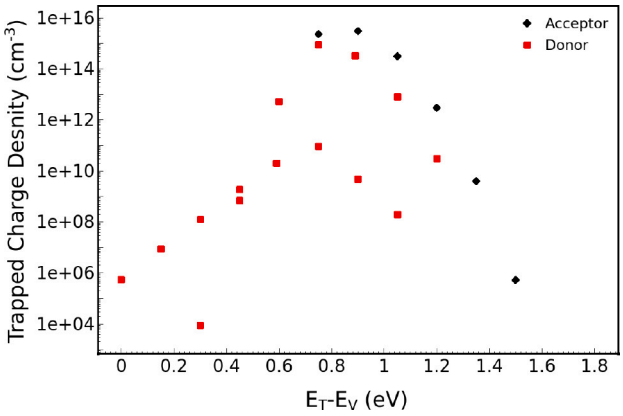

Fig. 3. Resulting trapped charge concentration within the a-Si:H material, as a result of trap density and trap occupation probability.

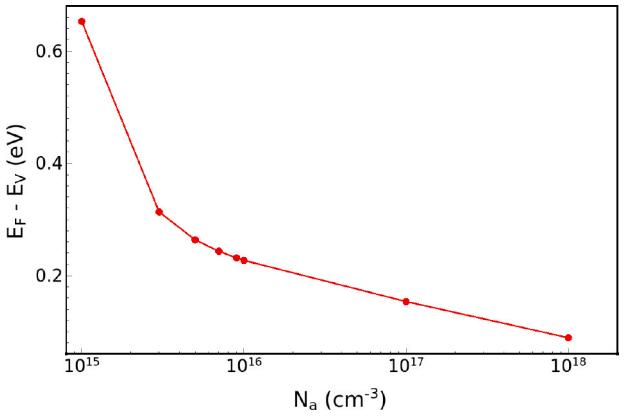

Fig. 4. Effect of the trapped charge concentration/effective doping concentration of the Fermi's level position. Arbitrarily high acceptor dopant concentrations have been considered.

level position. The resulting picture of trapped carriers, affecting the electrical behaviour of the device, is eventually reported in Fig. 3. Due to the material very low intrinsic concentration, even very low trapped charge concentrations cannot be neglected (i.e. in the order of $10^{3\div4}$ cm^{-3}). Namely, even traps with low densities with high occupation probabilities or traps with high concentrations and low occupation probabilities have to be taken into account. The effect of traps on some physical models can be modelled in an approximate manner by treating trap concentration as additional doping. Actually, the doping concentration is also affected including trap specifications with the *Add2TotalDoping* keyword. When *Add2TotalDoping* is specified, the trap concentration is added to both the acceptor or donor doping concentration (depending on the sign of the trap) and the total doping concentration. This affects models that depend on acceptor, donor, and total doping concentrations such as mobility and lifetime.

In this framework, with respect to crystalline silicon, the location of the Fermi's level is complicated because of the inherent defect states of the material (and therefore how it was grown up). In addition, Urbach's tail can also make a contribution [12]. It is therefore difficult to give an estimate of effective doping. The densities of states in the gap have been measured in the literature even with the variation of doping but only in rather fine films and their interfaces with crystalline silicon, to be used in photovoltaics application [13,14]. The resulting positions of the Fermi's levels are depicted in Fig. 4. The effect of an equivalent p-type substrate doping can be reproduced, considering the shift of the Fermi's level towards the valence band. The evidence of the localization of the position in the lower portion of the band gap can be reasonably reproduced with the increased concentration of the acceptor trap levels, which is in agreement with literature findings reported in [14]. The trap's introduction rate effects on Fermi's level position can also be evaluated, by considering its shift as a result of variation of the introduction factor, as reported in Fig. 5.

The main focus of this work deals however with the modelling of the carriers mobility within the device. In order to reproduce the macroscopic behaviour in terms of I-V at different temperatures, we devised a new carriers mobility model, starting from the Poole–Frenkel model available within Synopsys Sentaurus. Most organic semiconductors have mobilities dependent on the electric field. Sentaurus sdevice supports mobilities having a square-root dependence on the electric field, which is a typical mobility dependence for organic semiconductors and can be suitable in principle for amorphous silicon as well. The mobility as a function of the electric field is given by:

$$\mu = \mu_0 exp\left(-\frac{E_0}{kT}\right) exp\left(\sqrt{F}\left(\frac{\beta}{T}-\gamma\right)\right)$$

where μ is the low-field mobility, β and γ are fitting parameters, E_0 is the effective activation energy, T is the absolute temperature, k is the Boltzmann constant and F is the driving force (electric field).

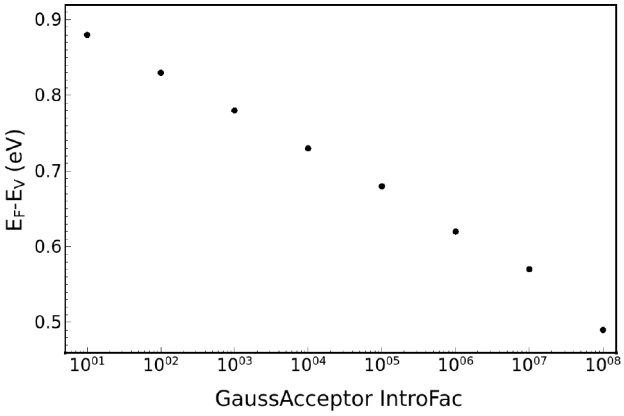

Fig. 5. Fermi's level position variation as a function of the traps introduction rates.

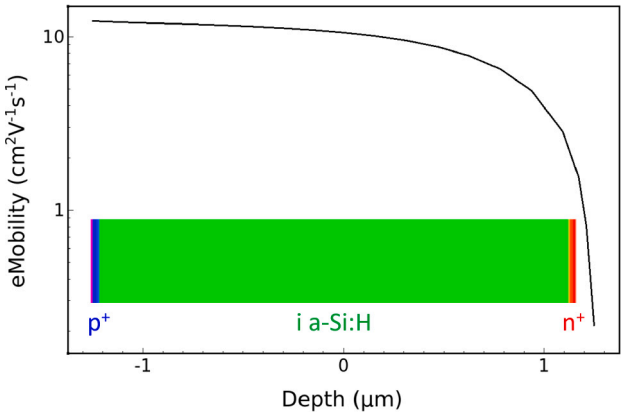

Fig. 6. Carriers mobility map within a reference p-i-n device on kapton.

However, the straightforward application of the Poole–Frenkel model cannot reproduce the increasing trend of the measured currents versus applied voltage and temperature. We therefore devised different custom mobilities models, to be included within the TCAD tool. Thanks to the Physical Model Interface (PMI) module, an advanced additional tool provided in Sentaurus sdevice, it is possible to embed within the Sentarus tools user-defined physical models to express many physical properties [8].

In particular, we considered an explicit dependence of the mobility on the potential and temperature, in addition to the exponential

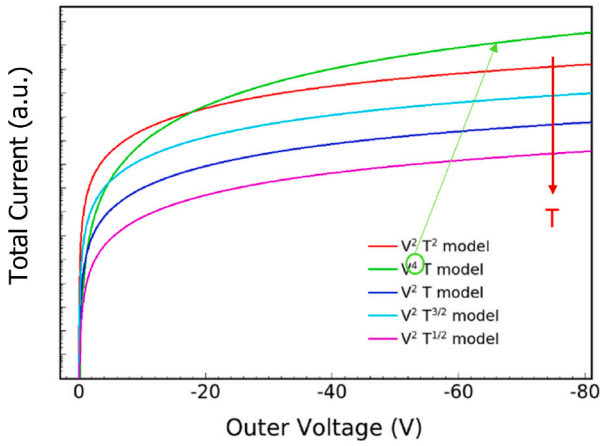

Fig. 7. Simulated I-V curves at different potential and temperature dependencies (T=300K).

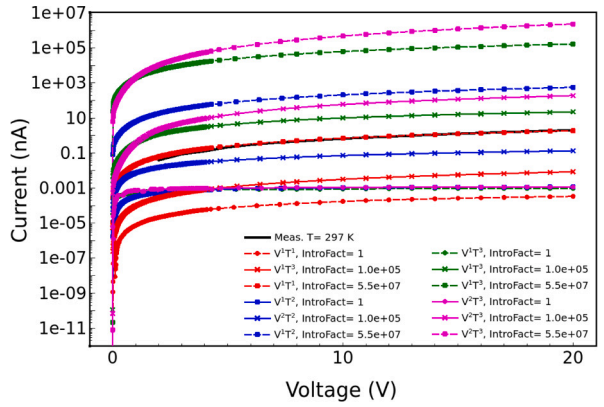

Fig. 8. Simulated I-V curves vs. measurements (20 °C): effects of temperature, voltage and introduction factor.

dependencies of the original Poole–Frenkel model. The dimensional consistency of the equation is guaranteed thanks to the introduction of suitable fitting parameters. The resulting mobility is given by

$$\mu = A^* V^m T^n exp\left(b\frac{\sqrt{|F|}}{T}\right)$$

where V is the internal electrostatic potential, A^* and b are fitting parameters, and F is the driving force (electric field). The m and n have been varied aiming at the best fit of the I-V measured curves at different temperatures.

Dependencies of the mobility on device characteristics, such as doping profiles and internal electric field distribution can be therefore taken into account, as depicted if Fig. 6. The macroscopic effect of the different dependencies of the mobilities on the internal potential (and therefore on the external biasing) and on temperature, resulting in different total currents, is reported in Fig. 7. As expected, the effect of external bias can be accounted for by increasing the exponent m of the ElectrostaticPotential (V), thus affecting the curvature of the curves. The increase of the temperature sensitivity (i.e., the exponent n) acts as an upper shift of the total current amount. The combined effects of temperature and electrostatic potential on the mobilities and the traps introduction rates are reported in Fig. 8. An excellent agreement with the experimental results can be obtained when unique scaling factors were applied to the concentration of individual acceptor/donor defects in the tails and Gaussian distribution of defects.

Different current transport models have been compared, from the classic drift-diffusion to the thermodynamic model accounting for self-heating, and eventually the hydrodynamic one accounting for energy transport of the carriers. However, no significant effects have been obtained with respect to the default drift-diffusion approximation, which has been therefore considered in this work.

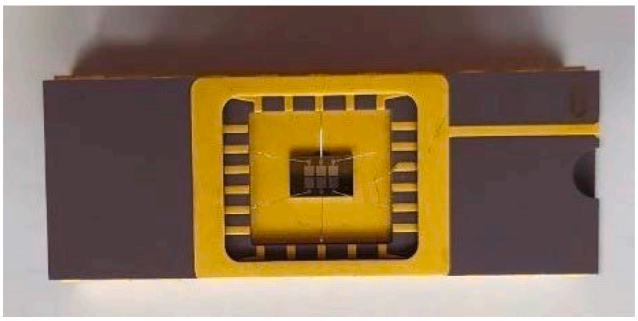

Fig. 9. p-i-n devices on crystalline silicon.

3. Device simulations vs. experimental measurements

In order to validate the proposed model and strategies, experimental findings have been considered as a reference. Simple test structures, featuring p-i-n diodes fabricated on different substrates have been simulated and compared to experimental data as a benchmark. In particular, p-i-n with different areas (0.25 mm^2 and 1 mm^2) deposited on crystalline silicon (c-Si) and p-i-n with different areas (16 mm^2 and 4 mm^2) deposited on Kapton have been used.

Measurements of dark current and capacitance versus bias voltage have been carried to evaluate the quality of the junction produced in the fabrication of the two implementation solutions. Tests of the various samples produced have been carried out using the INFN-Perugia test setup. In particular, it includes a MPI semi-automatic probe station TS 2000-SE operating between −60 °C and 200 °C with vacuum equipped chuck, six (vacuum-held) probes for the various electrical measurements, an optical microscope and a camera system for probe aligning and electrical connection system to the measuring equipment made with triaxial cables. The electrical test equipment includes, among others, a Keithley K707 switching matrix, a Source Measure Units (Keithley 237, Keithley 236 and Keithley 2410) and Agilent 4284 A LCR metre for High Frequency measurements.

The overall aim was to account for the effect of different biasing conditions (namely, different electrical potential and electric field distribution within the device) and operating conditions (e.g. temperature) on the electrical characteristics of the device. It should be noted that all the simulations were carried out by reproducing the exact test measurement procedures, in terms of measure temperature and external bias sweep.

The pictures of the actual devices, along with the simulated 2D cross sections are reported in Figs. 9, 10, 11 and 12 respectively. Gaussian doping profiles have been considered for the upper n^+ and lower p^+ implants, with ideal ohmic contacts at both device ends.

For measurement purposes, sensors deposited on kapton were subjected to preliminary tests to evaluate the potential damage caused by light exposure and the possible recovery of performance after an annealing process.

Actually, even freshly assembled sensors exhibit significantly lower sensitivity than expected if not properly stored in dark conditions. It turned out that just 20 min of ambient light is enough to reduce the sensor response by about 37% and to compromise its stability. To this respect, an initial annealing process was performed (12 h at 100 °C) to restore the expected sensitivity. Since the optimal annealing recipes are not yet known (i.e. how long it takes to maximize the performance or what the best performance is), it was decided to perform a second

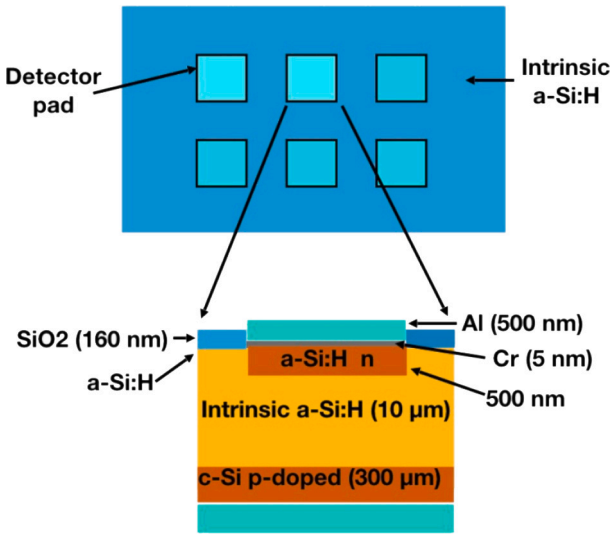

Fig. 10. p-i-n devices on crystalline silicon: simulated cross section.

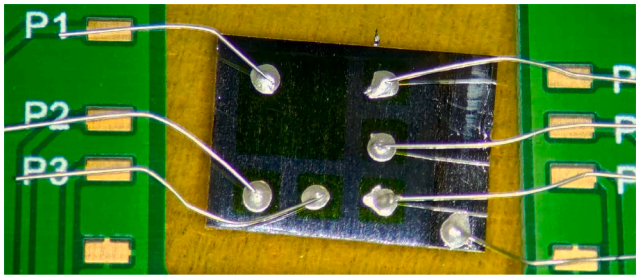

Fig. 11. p-i-n devices on kapton.

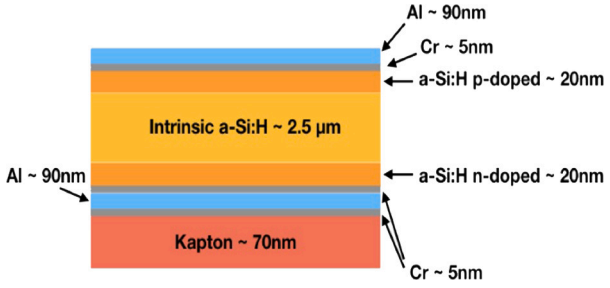

Fig. 12. p-i-n devices on kapton: simulated cross section.

annealing (12 h at 100 °C) and also consider auto-annealing, i.e. leaving the sensor in the dark for three weeks and then repeating the measurements.

Eventually, by properly setting the traps introduction rate, it was possible to reproduce the detector behaviour in a wide range of operating voltages and temperatures, as reported in Figs. 13 and 14.

In particular, by setting the parameters m and n a more than satisfactory agreement has been obtained for sensing devices operating conditions, in particular above 50 V and high temperature for thicker devices fabricated on crystalline substrates (Fig. 13) and above 10 V and room temperature for thin devices fabricated on kapton substrates (Fig. 14).

It should be mentioned that 2D simulation results have been successfully scaled to actual measurements by considering a proper area factor, i.e. the ratio between the actual device area and the area of the simulated domain. The overall agreement obtained with different

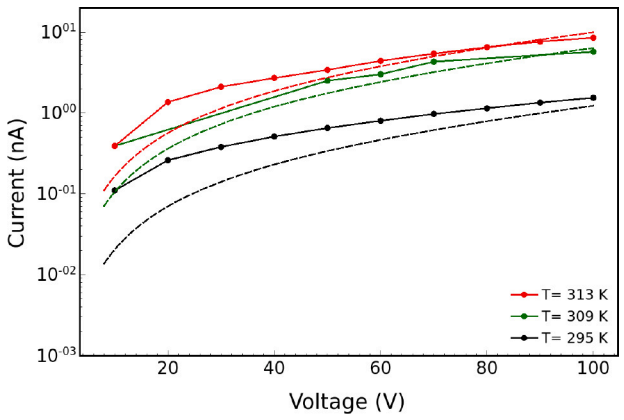

Fig. 13. I-V curves: simulations (dashed lines) vs. measurements (solid lines) at different temperatures for devices fabricated on crystalline substrates (PAD 1×1 mm^2).

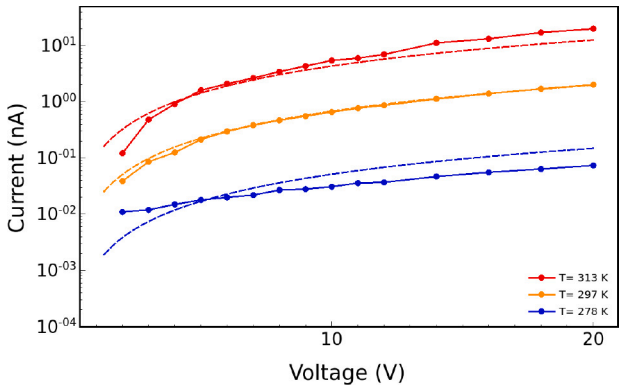

Fig. 14. I-V curves: simulations (dashed lines) vs. measurements (solid lines) at different temperatures for devices fabricated on kapton substrates.

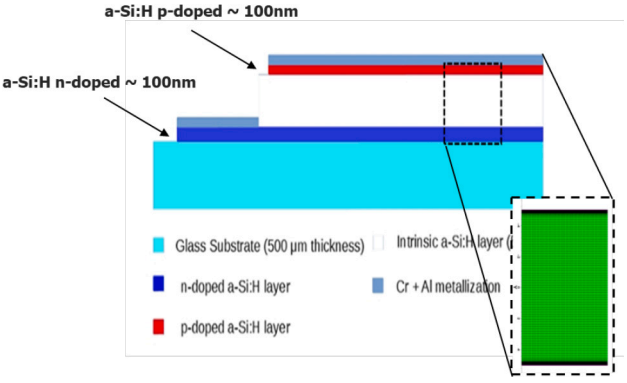

Fig. 15. p-i-n devices on glass: simulated cross-section.

devices, e.g. different geometries and fabrication processes, is a good indication of the predictivity of the model.

A further investigation has been carried out in order to evaluate the parametrization of the material. To this purpose, small-signal (AC) analyses have been carried out at different frequencies in order to simulate the C-V characteristics on a third class of devices, i.e. diode on glass depicted in Fig. 15. As reported in Fig. 16, an almost flat trend has been obtained thus indicating the lack of depletion of the reverse-biased junction with increasing biasing. Namely, the device acts as a quasi-linear capacitor, has inferred from actual C-V measurements.

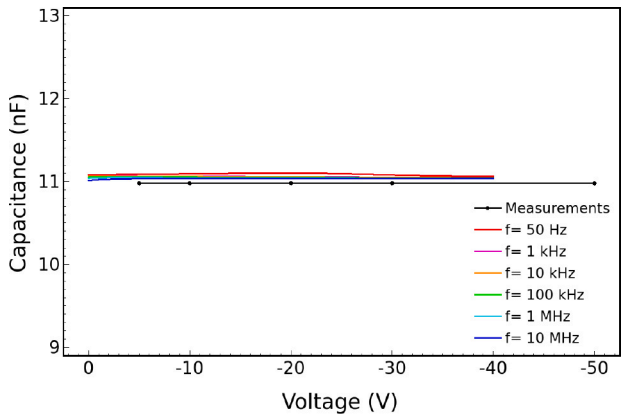

Fig. 16. C-V simulations vs. measurements: p-i-n devices on glass.

4. Conclusions

In this work, a novel approach to the modelling of hydrogenated amorphous silicon (a-Si:H) for particle detection applications has been proposed. A new material parametrization within the Sentaurus TCAD material library has been included. An extensive selection of acceptor and donor defects (acting as traps and/or recombination centres) within the band-gap has been considered, along with different options of energy distributions. Multiple acceptor/donor defects characteristic of the quasi-continuous conduction and valence tail states and the Gaussian mid-gap states have been introduced. Moreover, different custom mobility models have been devised and implemented within the code as external PMI (Physical Model Interfaces), starting from the Poole–Frenkel model and accounting for different dependencies on temperature and internal potential distribution, thus resulting in a new mobility model embedded within the code. Simple test structures, featuring p-i-n diodes have been simulated and compared to experimental data as a benchmark. The overall aim was to account for the effect of different biasing conditions (namely, different electrical potential and electric field distribution within the device) and operating conditions (e.g. temperature). Capacitance vs. voltage small-signal simulations and measurements analyses have been carried out to validate the model parametrization, while current vs. voltage simulations and measurements comparison has been used to check the suitability of the proposed charge transport and mobility models.

This work fosters the use of commercially available TCAD suites such as Synopsys Sentaurus, largely diffused in the radiation detection scientific community. This approach presents some advantages for the optimization of a radiation detector: the model is portable, reproducible and expandable to include further properties or parameters in the simulation of the device.

In particular, the proposed modelling approach overcomes the limitations pointed out in [3] without the need for a macroscopic ex-post fitting procedure, thanks to the extended validity range of carriers mobility models in terms of external biasing and high field, both typical operating conditions of particle detectors to be used in radiation damage environments such as High Energy Physics experiments.

To this extent, Synopsys TCAD provides the means to tune the models to achieve an acceptable accuracy while still maintaining perspective capabilities over different technological and layout options. Furthermore, it provides the additional advantage of simulating 2D or even 3D models of the device. This feature enables a better understanding of the effects on electric field distribution and on the charge collection efficiency created by specific geometries, relative position and dimensions of the electrodes which is of paramount importance for fine-tuning a position sensitive ionizing radiation detector. Transient analysis of single, minimum ionizing particles can be performed as well, accounting for the effect of radiation damage both at silicon interfaces and silicon bulk which are of paramount importance in medical, space or High-Energy Physics environments.

CRediT authorship contribution statement

Daniele Passeri: Conceptualization, Data curation, Investigation, Methodology, Writing – original draft, Writing – review & editing. **Arianna Morozzi:** Conceptualization, Data curation, Investigation, Methodology, Writing – original draft, Writing – review & editing. **Michele Fabi:** Writing – review & editing. **Catia Grimani:** Writing – review & editing. **Stefania Pallotta:** Writing – review & editing. **Federico Sabbatini:** Writing – review & editing. **Cinzia Talamonti:** Writing – review & editing. **Mattia Villani:** Writing – review & editing. **Lucio Calcagnile:** Writing – review & editing. **Anna Paola Caricato:** Writing – review & editing. **Maurizio Martino:** Writing – review & editing. **Giuseppe Maruccio:** Writing – review & editing. **Anna Grazia Monteduro:** Writing – review & editing. **Gianluca Quarta:** Writing – review & editing. **Silvia Rizzato:** Writing – review & editing. **Roberto Catalano:** Writing – review & editing. **Giuseppe Antonio Pablo Cirrone:** Writing – review & editing. **Giacomo Cuttone:** Writing – review & editing. **Giada Petringa:** Writing – review & editing. **Luca Frontini:** Writing – review & editing. **Valentino Liberali:** Writing – review & editing. **Alberto Stabile:** Writing – review & editing. **Tommaso Croci:** Writing – review & editing. **Maria Ionica:** Writing – review & editing. **Keida Kanxheri:** Writing – review & editing. **Mauro Menichelli:** Funding acquisition, Investigation, Methodology, Project administration, Writing – review & editing. **Francesco Moscatelli:** Writing – review & editing. **Maddalena Pedio:** Writing – review & editing. **Francesca Peverini:** Methodology, Formal analysis, Writing – review & editing. **Pisana Placidi:** Writing – review & editing. **Luca Tosti:** Methodology, Formal analysis, Writing – review & editing. **Giulia Rossi:** Writing – review & editing. **Leonello Servoli:** Funding acquisition, Investigation, Methodology, Project administration, Writing – review & editing. **Nicola Zema:** Writing – review & editing. **Giovanni Mazza:** Writing – review & editing. **Lorenzo Piccolo:** Writing – review & editing. **Richard Wheadon:** Writing – review & editing. **Luca Antognini:** Writing – review & editing. **Sylvain Dunand:** Writing – review & editing. **Nicolas Wyrsch:** Conceptualization, Data curation, Writing – review & editing. **Aishah Bashiri:** Writing – review & editing. **Matthew Large:** Conceptualization, Data curation, Writing – review & editing. **Marco Petasecca:** Conceptualization, Data curation, Writing – review & editing.

Declaration of competing interest

The authors declare that they have no known competing financial interests or personal relationships that could have appeared to influence the work reported in this paper.

Data availability

Data will be made available on request.

Acknowledgement

The HASPIDE project is funded by INFN through the CSN5 2021 Call.

References

[1] M. Menichelli, et al., Development of thin hydrogenated amorphous silicon detectors on a flexible substrate, 2022, http://dx.doi.org/10.48550/arXiv.2211.17114, arXiv:2211.17114v1 [physics.ins-det].

[2] M. Menichelli, et al., Fabrication of a hydrogenated amorphous silicon detector in 3-D geometry and preliminary test on planar prototypes, Instruments 5 (4) (2021) 32, http://dx.doi.org/10.3390/instruments5040032.

[3] J.A. Davis, M. Boscardin, M. Crivellari, L. Fanò, M. Large, M. Menichelli, A. Morozzi, F. Moscatelli, M. Movileanu-Ionica, D. Passeri, M. Petasecca, M. Piccini, A. Rossi, A. Scorzoni, B. Thompson, G. Verzellesi, N. Wyrsch, Modeling a thick hydrogenated amorphous silicon substrate for ionizing radiation detectors, Front. Phys. 8 (158) (2020) http://dx.doi.org/10.3389/fphy.2020.00158.

[4] W. Fuhs, L. Korte, M. Schmidt, Heterojunctions of hydrogenated amorphous silicon and monocrystalline silicon, J. Optoelectron. Adv. Mater. 8 (6) (2006) 1989–1995.

[5] C. Lee, H. Efstathiadis, J.E. Raynolds, P. Haldar, Two-dimensional computer modelling of single junction a-Si:H solar cells, in: 2009 34th IEEE Photovoltaic Specialists Conference, PVSC, Philadelphia, PA, 2009, pp. 001118–001122, http://dx.doi.org/10.1109/PVSC.2009.5411215.

[6] P. Otero, J.A. Rodriguez, M. Vetter, J. Andreu, E. Comesa na, A. Garcia Loureiro, A simulation of the temperature dependence of a-Si:H solar cell current–voltage characteristics, in: Spanish Conference on Electron Devices, Palma deMallorca, 2011, pp. 1–4, http://dx.doi.org/10.1109/SCED.2011.5744227.

[7] M. Nawaz, Design analysis of a-Si/c-Si HIT solar cells, Adv. Sci. Technol. 74 (2010) 131–136, http://dx.doi.org/10.4028/www.scientific.net/AST.74.131.

[8] Synopsys TCAD. Synopsys, 2013. Available online at: https://www.synopsys.com/silicon/tcad.html.

[9] M. Petasecca, F. Moscatelli, D. Passeri, G.U. Pignatel, Numerical simulation of radiation damage effects in p-type and n-type FZ silicon detectors, IEEE Trans. Nucl. Sci. 53 (2006) 2971–2976, http://dx.doi.org/10.1109/TNS.2006.881910.

[10] F. Moscatelli, et al., Combined bulk and surface radiation damage effects at very high fluences in silicon detectors: Measurements and TCAD simulations, IEEE Trans. Nucl. Sci. 63 (5) (2016) 7542192, 2716-2733.

[11] F. Moscatelli, et al., Effects of interface donor trap states on isolation properties of detectors operating at high-luminosity LHC, IEEE Trans. Nucl. Sci. 64 (8) (2017) 7935470, 2259-2267.

[12] Samer Aljishi, J. David Cohen, Shu Jin, Lothar Ley, Band tails in hydrogenated amorphous silicon and silicon-germanium alloys, Phys. Rev. Lett. 64 (23) (1990) 2811–2814, http://dx.doi.org/10.1103/physrevlett.64.2811.

[13] T.F. Schulze, C. Leendertz, N. Mingirulli, L. Korte, B. Rech, Impact of Fermi-level dependent defect equilibration on Voc of amorphous/crystalline silicon heterojunction solar cells, Energy Procedia 8 (2011) 282–287.

[14] L. Korte, M. Schmidt, Investigation of gap states in phosphorous-doped ultra-thin a-Si:H by near-UV photoelectron spectroscopy, J. Non-Cryst. Solids 354 (2008) 2138–2143.